Controllable Display of Sequential Enzymes on Yeast Surface with Enhanced Biocatalytic Activity toward Efficient Enzymatic Biofuel Cells

Shuqin Fan, Bo Liang, Xinxin Xiao, Lu Bai, Xiangjiang Tang, Elisabeth Lojou, Serge Cosnier, Aihua Liu

Controllable Display of Sequential Enzymes on Yeast Surface with Enhanced Biocatalytic Activity towards Efficient Enzymatic Biofuel Cells

Shuqin Fan [†,Σ,I], *Bo Liang*[Σ,I], *Xinxin Xiao* [†,I], *Lu Bai* [†], *Xiangjiang Tang*[Σ], *Elisabeth Lojou* [Δ,*], *Serge Cosnier* [ζ, η,*], *and Aihua Liu* [†,‡,*]

[†]Institute for Chemical Biology & Biosensing, and College of Life Sciences, Qingdao University, 308 Ningxia Road, Qingdao 266071, China

[‡]School of Pharmacy, College of Medicine, Qingdao University, 308 Ningxia Road, Qingdao 266071, China

[Σ]Qingdao Institute of Bioenergy & Bioprocess Technology, Chinese Academy of Sciences, 189 Songling Road, Qingdao 266101, China

[Δ]Aix Marseille Univ, CNRS, BIP, Bioénergétique et Ingénierie des Protéines UMR7281, 31 chemin Joseph Aiguier 13402 Marseille Cedex 20, France

[ζ] Université Grenoble-Alpes, DCM UMR 5250, F-38000 Grenoble, France

[η] Département de Chimie Moléculaire, UMR CNRS, DCM UMR 5250, F-38000 Grenoble, France

[I]These authors contributed equally to this work.

ABSTRACT

Precisely-localized enzyme cascade was constructed by integrating two sequential enzymes glucoamylase (GA) and glucose oxidase (GOx)) on yeast cell surface through a-agglutinin receptor as anchoring motif and cohesin-dockerin interactions. The overall catalytic activities of the combinant strains were significantly dependent on assembly method, enzyme molecular size, enzyme order and enzyme stoichiometry. The combinant strain with GA-DocC initially bound scaffoldin prior to GOx-DocT exhibited higher overall reaction rate. The highest overall reaction rate (29.28±1.15 nmol H_2O_2 min^{-1} mL^{-1}) was achieved when GA/GOx ratio was 2:1 with enzyme order: yeast-GA-GOx-GA, four-fold enhancement compared to free enzyme mixture. Further, the first example of starch/O_2 enzymatic biofuel cells (EBFCs) using co-displayed GA/GOx based bioanodes were assembled, demonstrating excellent direct biomass-to-electricity conversion. The optimized EBFC registered open-circuit voltage of 0.78 V and maximum power density (P_{max}) of 36.1 ± 2.5 μW cm^{-2}, significantly higher than the P_{max} for other starch/O_2 EBFCs reported so far. Therefore, this work highlights rational organization of sequential enzymes for enhanced biocatalytic activity and stability, which would find applications in biocatalysis, enzymatic biofuel cell, biosensing and bioelectro-synthesis.

INTRODUCTION

Sequential enzyme system consists of several enzymes, which can catalyze a cascade reaction,[1] *i.e.* the product of the first enzymatic reaction is the substrate for another or several subsequent reactions. However, randomly blending enzymes arise challenges such as enzyme activity loss and mismatch of the optimal condition of each enzyme, resulting in constrained overall activity. Enzyme cascades *in vivo* responsible for metabolism are metabolons,[2] in which cooperative enzymes are localized in separated organelles, enabling efficiently transporting of reactants between active sites to circumvent unfavorable equilibrium and kinetics. Inspired by natural metabolons, finely tailoring spatial configuration of sequential enzymes has been achieved by using polymers,[3] programmable DNA[4-6] and microbial surface display[7-8] to promote the overall catalytic efficiency, although the mechanism responsible for the accelerated efficiency is still under debate.[9-10] Among them, microbial surface display technology,[11-16] refering to the expression of enzymes on the surface of microbial cells, attracts considerable research interest as a powerful tool for surface modification of living microorganisms. The as-developed whole cell biocatalysts have natural advantages in multiple enzymes involved chemical reactions.[17-18] Unfortunately, proteins have been randomly displayed on the cell surface in most co-display systems so far, resulting in unsatisfying overall conversion efficiency.[19-20]

Enzymatic biofuel cells (EBFCs) use enzymatic catalysts to extract electricity from the chemical energy of fuel such as glucose and ethanol, etc.[21-32] As an inexpensive alternative, starch is widely available from plants. Starch is a polysaccharide containing numerous glucose units connected with glycosidic bonds. No single enzyme is capable of directly catalyzing starch oxidation. This redox transformation requires glucoamylase (GA) to catalyze the cleavage of the α-1, 4 and α-1, 6 glycosidic bonds to release glucose, which can be oxidized into gluconolactone by glucose dehydrogenase (GDH), or by glucose oxidase (GOx). However, co-immobilization of two or three enzymes on one electrode without precise localization does not favor appropriate space orientations of enzymes for the highest catalytic rate. In that context, ratio of enzymes is also expected to greatly influence the overall catalytic efficiency. As an illustration, Alfonta et al. displayed GA and GOx on yeast surfaces respectively,[7] without controls of their molecular ratio and localization. The resultant two-chamber starch/O_2 EBFC exhibited a maximum power density (P_{max}) of only ca. 3 μW cm^{-2},[7] which was likely the result of low catalytic efficiency arising from the spatial barrier between GA and GOx.

[Insert **Scheme 1**]

Scheme 1. (A) Schematic representation and the corresponding 3D structure for the co-display of sequential enzyme GA/GOx on bifunctional scaffold displayed on the yeast surface. Enzyme ratios of GA to GOx are 1:1 (EBY-C_1T_1-GA-GOx), 2:1 (EBY-$C_1T_1C_1$-GA-GOx, EBY-C_2T_1-GA-GOx) and 3:1 (EBY-$C_2T_1C_1$-GA-GOx). (B) 3D structures of GA, GOx, CohC-DocC and CohT-DocT complexes. The red and blue colored sticks refer to the active center of GA and GOx, respectively.

Herein, in a controllable manner, GA and GOx were co-displayed on the yeast cell surface *via* cohesin-dockerin interactions for rational enzyme cascade construction (**Scheme 1A**), in view of improving the catalytic efficiency.[33] The affinity of the binding between cohesin and dockerin is generally very high as indicated by previous studies[34-35]. The affinity is generally not affected by the fused enzyme and the linker, and these modules have been widely used for the fusion with different enzymes in various hosts.[13, 36] Since enzymes are on a microbial cell surface mimicking their natural environment[37], their stability is expected to be greatly enhanced.[7, 38-43] Further, three main factors i) enzyme assembling sequence which involves the overlapping of the optimal pH for GA and GOx, ii) enzyme order and iii) the enzyme stoichiometry, have been taken into consideration for optimization of flux balancing.[9] A typical activity assay was first employed to evaluate the catalytic efficiency of the surface displayed sequential enzyme system. Finally, as a proof of concept for direct biomass-to-electricity conversion, the microbial surface co-displayed sequential enzyme system was immobilized on solid electrodes as bioanodes coupled with a laccase (Lac) biocathode for oxygen reduction reaction to construct high performance starch/O_2 EBFCs (**Figure 3A**).

METHODS

Yeast Cell Surface Display of Scaffoldins and Secreted Expression of Dockerin-Fused Enzymes. To realize surface display of synthetic scaffoldins on *S. cerevisiae* EBY100, the yeast harboring various plasmids were precultured in SD-trp (glucose) medium for 24 h at 30 °C, and then precultures were subinoculated into SD-trp (galactose) medium at an optical density @ 600 nm (OD_{600nm}) of 1.0 and grown for 72 h at 25 °C. Yeast cells displaying synthetic scaffoldins on the surface were harvested. A portion of cells was washed with phosphate buffered saline (PBS),

and incubated for 4 h in PBS (0.2 mL) containing bovine serum albumin (BSA, 1 mg mL^{-1}) and anti-c-His immunoglobulin G (IgG, Invitrogen) with 400-fold dilution. Subsequently, the samples were washed and resuspended for 2 h in PBS (containing 1 mg mL^{-1} BSA and Flur 488-conjugated anti-mouse IgG (400-times dilution)). After washing three times with PBS, the cells were resuspended in PBS to an OD_{600nm} = 0.5 and characterized by fluorescence microscopy (Olympus BX51). X-33 strains expressing GA-DocC and GOx-DocT fusion proteins were precultured overnight at 30 °C in BMGY medium. The precultures were subinoculated into BMMY medium with 1% methanol and 10 mM $CaCl_2$ at an OD_{600nm} =1.0 and grown at 20 °C. After five days, the cultures were collected by centrifugation at 4 °C. The secreted expression enzymes were analyzed by 12% (wt/vol) SDS-polyacrylamide gel electrophoresis (SDS-PAGE). The concentration of crude enzyme extracts was determined by Bradford method.

Sequential Enzyme System Assembly on the Yeast Cell Surface. To check the functionality of individual assembly, the dockerin fusion enzymes were separately incubated with yeast cell surface displayed scaffoldin for 2 h using varying amounts of crude enzyme extracts at 4 °C. Then, the obtained cells were washed and resuspended in the assay buffer. GA and GOx activities of whole cell were determined. To investigate the effect of binding sequence of the chimeric enzyme on the efficiency of cascade reaction, the saturating amounts of dockerin-fused GA (dockerin-GA) or dockerin-fused GOx (dockerin-GOx) were mixed with cells displayed scaffoldins CohC-CohT, CohC-CohT-CohC and CohC-CohC-CohT-CohC, respectively. Yeast cell concentration was OD_{600nm}=1, with a total protein concentration of 0.11 and 0.14 mg mL^{-1} for GA-DocC and GOx-DocT, respectively. After incubation at 4 °C for 2 h, the cells were washed two times and then mixed with dockerin-GOx or dockerin-GA for another 2 h. Through the two-step assembly, the overall reaction rate was determined. In order to assemble sequential enzyme system using one-step process, the yeast cells displayed scaffoldins were mixed with the saturating amounts of enzymes for 4 h at 4 °C. The overall reaction rate was measured.

Preparation of Modified Bioanode and Biocathode. The glassy carbon electrode (GCE, diameter of 3 mm) was polished to a mirror finish carefully using 0.05 μm alumina slurries, and sonicated in water and anhydrous ethanol, respectively. Then, the electrode was thoroughly rinsed with deionized water and dried at room temperature. A 5 μL of poly(acrylic acid)-graphene dispersion was cast on the inverted electrode, and dried in air to acquire modified graphene/GCE.

For the preparation of bioanode, 5 μL aqueous dispersion of yeast displayed biocatalyst was added to the modified graphene/GCE, and dried in the fridge (4 ºC) overnight. Then 5 μL of Nafion solution (0.05 wt %) was syringed to the electrode surface to cover the electrode. For the modification of biocathode, 5 μL Lac (7.5 mg mL^{-1}) aqueous dispersion was coated on the graphene/GCE, and subsequently, 5 μL of Nafion solution (0.05 wt%) was dropped onto the surface of the resulting electrode, then dried in the fridge (4 ºC) overnight. The thus-prepared electrode was denoted as Lac/graphene/GCE.

Assembly of Biofuel Cells. The starch/O_2 EBFCs were assembled separately in two compartments. The anolyte was 0.2 M McIlvaine buffer (pH 5.0) containing 0.5 mM MB and 1.0% (w/w) starch. The catholyte was oxygen-saturated 0.2 M McIlvaine buffer (pH 5.0) containing 0.5 mM of ABTS. The cation exchange membrane was used to separate the anodic and cathodic compartments. In a control experiment, the power curves in the absence of displayed enzymes but with the redox mediators in solution were performed by assembling an EBFC using yeast/graphene/GCE as anode and Lac/graphene/GCE as cathode. Fuel cell experiments were performed by recording a linear sweep polarization at a scan rate of 1 mV s^{-1} with the anode connected to the counter and reference leads, and the cathode connected to the working lead. Power densities were obtained by normalizing the power by the surface area of the limiting electrode.

RESULTS AND DISCUSSION

Controllable Design and Construction of Scaffoldin Yeast Surface Display Systems. The assembly of GA and GOx onto scaffoldin was achieved by cohesin-dockerin interaction (**Scheme 1B**). CohC and DocC originated from *Clostridium cellulolyticum*, while CohT and DocT from *Clostridium thermocellum* (Supporting Information, Experimental methods, in which the recombinant strains and plasmids as well as primers are listed in **Table S1** and **S2**). Dockerin was fused to the C-terminal of the enzyme. There were no linkers in between of GA and DocC, GOx and DocT. α-Factor secretion signal peptide was used for directing secreted expression of the recombinant protein. In order to display chimeric scaffold protein containing CohC and CohT domains of different specificity on the cell surface of yeast, the a-agglutinin receptor, consisting of two subunits encoded by the *AGA1* and *AGA2* genes was used as an anchoring motif. This receptor has been proved to facilitate yeast surface display of GOx in a previous study.[44] Successful

expressions of dockerin-GA and dockerin-GOx in yeast were confirmed by SDS-PAGE analysis (**Figure 1**). The expected 63 kDa band was detected in cultures containing GA-DocC. The molecular weights of mature GOx and DocT were 64 kDa and 7.5 kDa, respectively, according to their amino acid sequences (**Table S3**). The higher molecular weight of GOx-DocT (97 kDa) was probably contributing from 41.7% glycosylation of GOx from *P. pastoris*.[45] No target protein bands were detected in the supernants of non-induced cultures. Activities of the recombined GA and GOx were 4.55±0.05 and 4.40±0.04 U/mg total protein, respectively, confirming their proper protein folding and considerable activity. The correct location of the scaffoldin and the successful integration of scaffoldins on the yeast surface were confirmed by immunofluorescence analysis, from which bright fluorescence was observed for the cells harboring recombinant plasmids, in contrast to the negative control cells non-displaying scaffoldin (**Figure S1,** Supporting Information).

[Insert **Figure 1**]

Figure 1. SDS-PAGE analysis of yeast surface displaying various fusion proteins. Lane M, protein standard markers. Culture supernatants of X33-GOx before (Lane a) and after (Lane b) induction. Culture supernatants of X33-GA before (Lane c) and after (Lane d) induction.

GA and GOx Assembling on the Yeast Surface via Unifunctional System. To test whether unifunctional system could be assembled onto the yeast cell surface, the fusion enzymes were separately incubated with yeast-expressing scaffoldin with different amounts of enzymes. After the same period of incubation, cells were washed twice to remove any unbounded proteins. Initially, the activity increased with the increasing amounts of each enzyme, and subsequently leveled off (**Figure 2)**, suggesting that the cohesin was saturated with suitable dockerin-fused enzyme. When the ratio of CohC to CohT was 1:1, the amount of saturated GA-DocC and GOx-DocT were 85 μg and 260 μg, respectively. GA-displayed strain could generate about 2689 μmol L^{-1} h^{-1} glucose when yeast cell was incubated with 1% starch at 30 °C while continuing shaking at 250 rpm for 1 h. A previous study reported yeast cell surface displayed GA from *A. niger* could produce 2496 μmol L^{-1} h^{-1} glucose under the same conditions[7]. The different activities were probably due to the different display mechanisms and the GA source of species. Meanwhile, the GOx activity of the GOx-displayed strain was also tested. The activity was 0.16±0.005 U/OD_{600nm} using 1.72% glucose as the substrate, which was similar to that of yeast cells displaying GOx using

a-agglutinin as the anchoring motif.[44] Furthermore, when enzymes assembled on EBY-$C_1T_1C_1$, the amount of GA-DocC increased almost one-fold, while that of GOx-DocT was unchanged. However, the amounts of saturated enzymes were declined when the ratio of CohC to CohT continued to increase. The number of GOx-DocT decreased is likely due to the increased molecular size of expressed cohesin scaffold posed more metabolic burden on the strain, which may lower the display efficiency.

[Insert **Figure 2**]

Figure 2. Binding curves for each dockerin-GA (A) and dockerin-GOx (B) on EBY-C_1T_1, EBY-$C_1T_1C_1$ and EBY-$C_2T_1C_1$. The protein concentration was 0.11 and 0.14 mg mL^{-1} for GA-DocC and GOx-DocT, respectively.

Controllably Co-Displaying Sequential Enzyme GA and GOx via Bifunctional System and Their Biocatalytic Efficiencies. The sequential enzyme system in this work was further constructed by incubating yeast cells displaying the bifunctional scaffoldin with a saturating level of two enzymes (**Figure 2**). It is worthy of note that the overall reaction rate was sensitive to the assembling sequence of GA-DocC and GOx-DocT onto the chimeric scaffold (**Table 1**). Specifically, when the fusion protein GA-DocC was first bound onto the scaffoldin CohC-CohT, the complex showed considerable overall reaction rate and reached 13.16±0.81 nmol H_2O_2 min^{-1} mL^{-1}. On the contrary, when the order of the assembly was reversed, the overall reaction rate was decreased by 26%. Besides, nearly 14.8% of the overall reaction rate was lost when GA-DocC and GOx-DocT were simultaneously loaded onto the chimeric scaffold. The different catalytic efficiencies might originate from the different size of the two enzymes. Being active as a dimer, GOx (ca. 194 kDa) is much larger than GA (ca. 64 kDa), and steric hindrance could prevent the assembly of GA onto the scaffoldin in the presence of GOx. Free enzyme mixtures, in which enzymes did not orient to be seated in the scaffold, were used as controls. The amounts of enzymes in free enzyme mixtures were kept consistent with those in "whole cell catalysis" based on the saturation binding curves (**Figure 2**). Free enzyme mixtures showed a similar overall reaction rate irrespective of assembly sequences, however, with only 55% of the value observed for GA/GOx co-displaying cells. The different performances indicate that the controlled

positioning of enzymes, *i.e.* satisfying enzyme-substrate proximity and enzyme-enzyme proximity, could enhance the metabolic flux to improve the overall reaction rate.[1, 46-48]

Table 1. Comparison of overall reaction rate of sequential enzymes assembled on EBY-C_1T_1 by different assembly methods.

Assembly methods	Overall reaction rate [a] (nmol H_2O_2/min/mL)	
	Whole cell catalyst	Free GA and GOx mixture
GA-DocC+GOx-DocT [b]	11.21±0.72	7.31±0.43
GA-DocC→GOx-DocT [c]	13.16±0.81	7.25±0.45
GOx-DocT→GA-DocC [d]	9.74±0.63	7.29±0.57

[a]The values shown represent the average of three repetitive measurements plus-minus standard deviation; [b]Both GA-DocC and GOx-DocT loaded onto the chimeric scaffoldin simultaneously; [c]GA-DocC was first bound onto the scaffoldin prior to GOx-DocT; [d]GOx-DocT was first bound onto the scaffoldin prior to GA-DocC.

Subsequently, the effect of enzyme order on the overall reaction rates was investigated for a GA/GOx ratio of 2:1. Two types of combinant strains of EBY-$C_1T_1C_1$-GA-GOx and EBY-C_2T_1-GA-GOx were examined considering that the larger molecular size for GOx (**Scheme 1**). It was found that the overall reaction rate was 29.28±1.15 nmol H_2O_2 min^{-1} mL^{-1} for EBY-$C_1T_1C_1$-GA-GOx and 22.32±1.06 nmol H_2O_2 min^{-1} mL^{-1} for EBY-C_2T_1-GA-GOx. In other words, the overall reaction rate for EBY-C_2T_1-GA-GOx was 23.8% lower than that value for EBY-$C_1T_1C_1$-GA-GOx, suggesting the influence from the order of the displayed enzymes.

In the present cascade reaction, the rate-limiting step is the hydrolysis of starch by GA, which presents a lower affinity towards its substrate and a slower turnover rate than GOx.[49-50] Therefore, the ratio of GA to GOx on cell surface should be a crucial factor. Thus, different GA/GOx ratios (1:1 (EBY-C_1T_1-GA-GOx), 2:1 (EBY-$C_1T_1C_1$-GA-GOx) and 3:1 (EBY-$C_2T_1C_1$-GA-GOx)) were designed to be co-displayed on yeast surface, with the expectation that an increased enzyme ratio could enhance the overall catalytic efficiency. To achieve this, chimeric scaffoldins with different CohC:CohT ratios (1:1, 2:1 and 3:1) were prepared (**Scheme 1**). The ratio of GA to GOx on the cell surface was optimized by regulating the relative amounts of CohC and CohT domains. Similar to the above co-display system, two enzymes were assembled on strain EBY-$C_1T_1C_1$ and EBY-

$C_2T_1C_1$, respectively. To get a control of the molecular ratio of GA to GOx on the cell surface, the number of expressed enzyme units on the bifunctional yeast cell surface was determined. The calculated ratio of GA to GOx units on the yeast cell surface was in line with expectations (**Table S4**, Supporting Information). The overall reaction rate reached the maximum value (29.28±1.15 nmol H_2O_2 min^{-1} mL^{-1}) for EBY-$C_1T_1C_1$-GA-GOx (with a GA/GOx ratio of 2:1), which fell to 20.04±0.98 nmol H_2O_2 min^{-1} mL^{-1} for EBY-$C_2T_1C_1$-GA-GOx (with GA/GOx ratio of 3:1). The result can be explained by the fact that large passenger proteins limited the efficiency of surface expression. It is noteworthy that there were about 72 000 GA-DocC enzymes per cell when the strain was EBY-$C_1T_1C_1$-GA-GOx, in comparison with 64 000 GA-DocC enzymes per cell for EBY-$C_2T_1C_1$-GA-GOx. Such decrease in the amount of surface displayed enzymes per cell was mainly because large passenger proteins limited the efficiency of surface expression. Other display systems showed similar trend, in which the size of the passenger protein influenced the efficiency of expression and surface display using pYD1 yeast display system.[13]

Storage Stability of the Co-Displayed Sequential Enzymes. The long-term stability of the biocatalysts has been monitored (**Figure S2**, Supporting Information). EBY-$C_1T_1C_1$-GA-GOx retained more than 90% of the original activity during the one-month period when yeast was incubated at 4 °C and room temperature. In contrast, the free enzyme mixture only retained 75% of the initial activity. The higher stability of recombinant strains compared to that of the free enzymes is mainly attributed to the yeast cell surface providing a biocompatible micro-environment, as demonstrated in our previous studies.[51]

Assembly of Starch/O_2 EBFCs. The co-displayed sequential enzymes were further immobilized on GCEs and employed as bioanodes of starch/O_2 EBFCs. Lac from *Trametes versicolor* adsorbed onto graphene/GCE (Lac/graphene/GCE) was used as the biocathode. Indeed, Lac is known to catalyze a 4-electron reduction of O_2 to water at a relatively high onset potential under an optimized pH in the region of 3-5.[52] To establish an efficient electrochemical communication between the electrode surface and enzymes' active centers, 0.5 mM methylene blue (MB) and 2,2'-azinobis (3-ethylbenzothiazoline-6-sulfonic acid) diammonium salt (ABTS) in aqueous solution were used separately as the electron transfer mediators for the bioanodes and Lac/graphene/GCE biocathodes (**Figure S3**). Two-compartment starch/O_2 EBFCs were assembled by using a cation exchange

membrane to separate the anodic and cathodic chambers. As illustrated in **Figure 3A**, the yeast surface co-displayed GA/GOx catalyzes the hydrolysis of starch and the subsequent glucose oxidation on the bioanode. Electrons generated by GOx-catalyzed glucose oxidation are transferred to electrode with the mediation of MB, and via the external circuit to the biocathode. The immobilized Lac uses the electrons from the bioanode to reduce O_2 to water using ABTS as the redox mediator (**Figure S3**).

[Insert **Figure 3**]

Figure 3. (A) Schematic drawing of electron transfer routes and catalytic reactions in the proposed two-compartment starch/O_2 EBFC. (B, C) Power density-voltage profiles of two-compartment starch/O_2 EBFCs on different bioanodes, which were fabricated by depositing biocatalysts onto graphene/GCE. 0.2 M McIlvaine buffer (pH 5.0) containing 0.5 mM MB and 1.0% (w/w) starch was used for the bioanode compartment, while the Lac/graphene/GCE was used throughout as the biocathode, in which O_2-saturated 0.2 M McIlvaine buffer (pH 5.0) with 0.5 mM ABTS was used for the biocathode compartment. Blank control (d) indicates a cell consisting of a yeast/graphene/GCE based anode and a Lac/graphene/GCE based cathode. (D) The summarized P_{max} of the starch/O_2 EBFC as a function of the anode catalyst.

Performance of the Starch/O_2 EBFCs. The power densities of starch/O_2 EBFCs as a function of yeast surface co-displayed GA/GOx ratios were evaluated (**Figure 3B**). The P_{max} increased from 21.4±1.7 to 36.1±2.5 μW cm^{-2} along with the increase of the ratios of co-displayed GA/GOx from 1:1 (EBY-C_1T_1-GA-GOx) to 2:1 (EBY-$C_1T_1C_1$-GA-GOx), suggesting that more GA molecules in the co-displayed GA/GOx result in higher P_{max}. This observation is in accordance with the limiting step of starch hydrolysis, in which the overall efficiency can be improved by increasing the proportion of GA. However, when the GA/GOx ratio was further increased to 3:1 (EBY-$C_2T_1C_1$-GA-GOx), the P_{max} of starch/O_2 EBFC declined slightly to 28.3 ± 2.3 μW cm^{-2} because the displayed enzymes reached saturation. The trend obtained here was in accordance with the observation of the overall reaction rate for the whole cell catalysts, in which the aforementioned biocatalysis activity of yeast displayed co-enzyme EBY-$C_1T_1C_1$-GA-GOx (GA/GOx ratio of 2:1) in free solution is 1.46-fold of that value of EBY-$C_2T_1C_1$-GA-GOx (GA/GOx ratio of 3:1), indicative of a bioanode-dependent EBFC. Moreover, the blank control cell consisting of

electrodes without biocatalyst loading showed a very poor P_{max} of 0.25 μW cm^{-2} and a quite narrow open circuit voltage (OCV) of 0.16 V when tested in the same solutions (curve d in **Figure 3B**, **Figure S4**). This result indicates that the considerable power and OCV obtained in the curves a-c of **Figure 3B** are due to the presence of biocatalysis process.

As controls, starch/O_2 EBFCs based upon GA-yeast & GOx-yeast (2:1)/graphene/GCE and free GA & free GOx (2:1)/graphene/GCE as bioanodes were also constructed. Their power densities towards 1.0% (w/w) starch are shown in **Figure 3C**. A high OCV of 0.78 V was observed for the starch/O_2 EBFC with EBY-$C_1T_1C_1$-GA-GOx as the anode catalyst. Further, the P_{max} of the starch/O_2 EBFC with co-displayed GA&GOx-yeast (n:1, where n is 2 and 3) as the anode catalyst was greatly higher than the power output achieved using GA-yeast *&* GOx-yeast(2:1) or free GA *&* free GOx (2:1) as the anode catalyst, respectively (**Figure 3C** and **Figure 3D**), although the amounts of free GA *&* free GOx (2:1), and GA-yeast *&* GOx-yeast (2:1) added to the bioanode were matched to EBY-$C_1T_1C_1$-GA-GOx based on calculation.

Table 2. Comparison of the performance of starch/O_2 EBFCs

Anode biocatalyst	Cathode biocatalyst	P_{max} (μW cm^{-2})	OCV (V)	Ref.
GA-yeast &GOx	Pt/C	0.8 ± 0.07	~0.48	[7]
GA-yeast&GOx-yeast	Pt/C	1.8±0.3	0.63	[7]
Free GA and GDH	bilirubin oxidase	1.7	0.53	[53]
Free GA and GOx	laccase	8.15	0.53	[54]
EBY-$C_1T_1C_1$-GA-GOx	laccase	36.1 ± 2.5	0.78	This work
EBY-$C_2T_1C_1$-GA-GOx	laccase	28.3 ± 2.3	0.74	This work
EBY-C_1T_1-GA-GOx	laccase	21.4±1.7	0.67	This work
GA-yeast & (2:1) GOx-yeast	laccase	23.6 ± 2.6	0.77	This work
Free GA& (2:1) free GOx	laccase	20.6 ± 1.4	0.72	This work

The P_{max} of the starch/O_2 EBFC with EBY-$C_1T_1C_1$-GA-GOx as the anode catalyst was 36.1 μW cm^{-2}, significantly higher than the power output achieved by the GA-yeast&GOx-yeast(2:1) (23.6 μW cm^{-2}) and the free GA & free GOx (2:1) (20.6 μW cm^{-2}) as the anode catalyst, respectively.

The performances of starch/O_2 EBFCs reported so far in the literature are summarized in **Table 2**. The EBFC with EBY-$C_1T_1C_1$-GA-GOx based bioanode also exhibited the highest short-circuit current density (62.7 μA cm^{-2}) among these tested EBFCs (**Figure S5**). Although the amount of immobilized enzymes may vary, the P_{max} of the GA-yeast & GOx-yeast based starch/O_2 EBFC was ca. 1.8 μW cm^{-2},[7] which is 1/20 of the value obtained in this work for the EBY-$C_1T_1C_1$-GA-GOx based EBFC. The co-immobilized free GA and GOx anode based starch/O_2 EBFC showed a P_{max} of 8.15 μW cm^{-2} and an OCV of 0.53 V.[39] The higher OCV obtained here is attributed to the low onset potential of GOx dependent bioanodes and high onset potential of the Lac based biocathode using ABTS as the redox mediator (**Figure S3B**). In contrast to the cell surface displayed system with controllable organization of sequential enzymes, the inferior P_{max} values for free enzyme mixtures of GA/GOx are mainly due to the negative influence of the uncontrollable ratio and uncertain spatial organization of sequential enzymes and the impact of these factors on substrate diffusion in the cascade reaction.[55-56] Conversely, enzymes with rational orientation on the scaffoldin undergo decreased intermediates diffusion to the bulk solution and enhanced intermediates channelling between different enzymes' active sites.[57]

Operational Stability of the EBFCs. A major issue in EBFCs is the short lifetime caused by a reduction in the stability and activities of oxidoreductases when extracting from their microorganism and functioning in a foreign environment.[58] To test the stabilities of the assembled starch/O_2 EBFCs, the cells were examined in as-prepared 1.0% (w/w) starch solution under O_2-saturated atmosphere with different anode catalysts, respectively. During a course of 30 h continuous operation, the starch/O_2 EBFC with EBY-$C_1T_1C_1$-GA-GOx as the bioanode catalyst showed the best stability with 69% of its original power remaining (**Figure 4**), higher than those of GA-yeast&GOx-yeast(2:1) (61%) and free GA & free GOx (2:1) (48%). In addition to the high power density (**Figure 3B**), the best operational stability was achieved for the EBFC with co-displayed GA and GOx sequentially on the cell based bioanode. The stable power output probably benefits from the biocompatibility, appropriate ratio and the controlled sequence of the enzymes co-displayed on the yeast surface. This was verified by monitoring the long-term stability (one month) of the un-immobilized cell surface displayed enzymes. The higher stability of the recombinant strains compared to that of the free enzymes is mainly attributed to the yeast cell

surface providing a biocompatible micro-environment, which has been demonstrated in our early studies where xylose dehydrogenases were displayed on the surface of *Escherichia coli*.[51]

[Insert **Figure 4**]

Figure 4. The normalized power output of different starch/O_2 EBFCs as a function of operation time.

CONCLUSIONS

In summary, sequential enzyme (GA/GOx)-displaying system was successfully constructed in controlling the assembly method, enzyme molecular size, enzyme order and ratio. This was achieved by i) displaying various chimeric scaffold proteins on the yeast cell, ii) expression of dockerin-GOx and dockerin-GA with considerable enzymatic activities and iii) binding of fusion proteins (GA-DocC and GOx-DocT) onto the cell surface displayed scaffolds *via* cohesin-dockerin interaction. The assembly sequence of the fused GOx and GA onto the scaffold, the enzyme order and co-displayed GA/GOx ratio determined the overall enzymatic activity. Starch/O_2 EBFCs were assembled using co-displayed GA&GOx based bioanodes and a laccase modified biocathode, allowing the direct conversion of abundant biomass into electricity. The starch/O_2 EBFC with an optimized EBY-$C_1T_1C_1$-GA-GOx based bioanode registered the largest OCV, the highest P_{max}, and also the most prominent stability. This is the first biofuel cell example to use co-displaying sequential GOx and GA on the surface of yeast as biocatalyst for efficient starch/O_2 EBFCs. It is envisioned that the controllably designed sequential enzyme displayed cell system would find a wide range of applications in the fields of biocatalysis, bioenergy, bioelectro-synthesis and biosensing.

ASSOCIATED CONTENT

Supporting Information

The Supporting Information is available free of charge at https://pubs.acs.org. Supplementary experimental methods: Strains, media and chemicals; Plasmid construction; Enzyme assays; Construction of EBFCs and their performance testing. Supplementary tables: Strains and plasmids;

PCR primers; Amino acid sequences of dockerin-fused proteins; The numbers of expressed enzyme units on the yeast cell surface. Supplementary figures: Immunofluorescence micrographs; Long-term stability assays; Biocathode characterization; Power density-voltage profile of the blank control cell; Polarization curves of starch/O_2 EBFCs.

AUTHOR INFORMATION

Corresponding Authors

***Elisabeth Lojou** − *Aix Marseille Univ, Marseille, France*; orcid.org/0000-0003-2593-4670; E-mail: lojou@imm.cnrs.fr.

***Serge Cosnie**r − *Université Grenoble-Alpes, and UMR CNRS, Grenoble, France*; orcid.org/0000-0002-8290-4374; E-mail: serge.cosnier@univ-grenoble-alpes.fr;

***Aihua Liu** − *Qingdao University, Qingdao, China*; orcid.org/0000-0003-4260-1982 E-mail: liuah@qdu.edu.cn.

Other Authors

Shuqin Fan − *Qingdao University, and Qingdao Institute of Bioenergy & Bioprocess Technology, Chinese Academy of Sciences, Qingdao, China*

Bo Liang − *Qingdao Institute of Bioenergy & Bioprocess Technology, Chinese Academy of Sciences, Qingdao, China*

Xinxin Xiao − *Qingdao University, Qingdao, China*

Lu Bai − *Qingdao University, Qingdao, China*

Xiangjiang Tang − *Qingdao Institute of Bioenergy & Bioprocess Technology, Chinese Academy of Sciences, Qingdao, China*

Complete contact information is available at: https://pubs.acs.org/10.1021/

Notes

The authors declare no competing financial interest.

ACKNOWLEDGMENTS

This work was financially supported by National Natural Science Foundation of China (No 21275152) to A.L., ANR (ENZYMOR-ANR-16-CE05-0024) to E.L. and platform Chimie

NanoBio ICMG FR 2607 (PCN-ICMG) to S.C. We thank Dr Zhiguang Zhu for helpful discussion.

REFERENCES

1. Kuchler, A.; Yoshimoto, M.; Luginbuhl, S.; Mavelli, F.; Walde, P., Enzymatic reactions in confined environments. *Nat. Nano.* **2016,** *11* (5), 409-420.
2. Zhang, Y.; Beard, K. F. M.; Swart, C.; Bergmann, S.; Krahnert, I.; Nikoloski, Z.; Graf, A.; Ratcliffe, R. G.; Sweetlove, L. J.; Fernie, A. R.; Obata, T., Protein-protein interactions and metabolite channelling in the plant tricarboxylic acid cycle. *Nat. Commun.* **2017,** *8*, 15212.
3. Vriezema, D. M.; Garcia, P. M.; Sancho Oltra, N.; Hatzakis, N. S.; Kuiper, S. M.; Nolte, R. J.; Rowan, A. E.; van Hest, J., Positional assembly of enzymes in polymersome nanoreactors for cascade reactions. *Angew. Chem. Int. Ed.* **2007,** *119* (39), 7522-7526.
4. Fu, J.; Liu, M.; Liu, Y.; Woodbury, N. W.; Yan, H., Interenzyme Substrate Diffusion for an Enzyme Cascade Organized on Spatially Addressable DNA Nanostructures. *J. Am. Chem. Soc.* **2012,** *134* (12), 5516-5519.
5. Ngo, T. A.; Nakata, E.; Saimura, M.; Morii, T., Spatially Organized Enzymes Drive Cofactor-Coupled Cascade Reactions. *J. Am. Chem. Soc.* **2016,** *138* (9), 3012-3021.
6. Xia, L.; Van Nguyen, K.; Holade, Y.; Han, H.; Dooley, K.; Atanassov, P.; Banta, S.; Minteer, S. D., Improving the performance of methanol biofuel cells utilizing an enzyme cascade bioanode with dna-bridged substrate channeling. *ACS Energy Lett.* **2017,** *2* (6), 1435-1438.
7. Bahartan, K.; Amir, L.; Israel, A.; Lichtenstein, R. G.; Alfonta, L., In situ fuel processing in a microbial fuel cell. *ChemSusChem* **2012,** *5* (9), 1820-1825.
8. Szczupak, A.; Aizik, D.; Moraïs, S.; Vazana, Y.; Barak, Y.; Bayer, E. A.; Alfonta, L., The electrosome: a surface-displayed enzymatic cascade in a biofuel cell's anode and a high-density surface-displayed biocathodic enzyme. *Nanomaterials* **2017,** *7* (7), 153.
9. Zhang, Y.; Hess, H., Toward rational design of high-efficiency enzyme cascades. *ACS Catal.* **2017,** *7* (9), 6018-6027.
10. Zhang, Y.; Tsitkov, S.; Hess, H., Proximity does not contribute to activity enhancement in the glucose oxidase–horseradish peroxidase cascade. *Nat. Commun.* **2016,** *7*, 13982.
11. Tsai, S. L.; Oh, J.; Singh, S.; Chen, R. Z.; Chen, W., Functional assembly of minicellulosomes on the *Saccharomyces cerevisiae* cell surface for cellulose hydrolysis and ethanol production. *Appl. Environ. Microbiol.* **2009,** *75* (19), 6087-6093.
12. Wen, F.; Sun, J.; Zhao, H. M., Yeast surface display of trifunctional minicellulosomes for simultaneous saccharification and fermentation of cellulose to ethanol. *Appl. Environ. Microbiol.* **2010,** *76* (4), 1251-1260.
13. Fan, L. H.; Zhang, Z. J.; Yu, X. Y.; Xue, Y. X.; Tan, T. W., Self-surface assembly of cellulosomes with two miniscaffoldins on *Saccharomyces cerevisiae* for cellulosic ethanol production. *Proc. Natl. Acad. Sci.* **2012,** *109* (33), 13260-13265.
14. Srikrishnan, S.; Chen, W.; Da Silva, N. A., Functional assembly and characterization of a modular xylanosome for hemicellulose hydrolysis in yeast. *Biotechnol. Bioeng.* **2013,** *110* (1), 275-285.
15. Liang, Y. Y.; Si, T.; Ang, E. L.; Zhao, H. M., Engineered pentafunctional minicellulosome for simultaneous saccharification and ethanol fermentation in *Saccharomyces cerevisiae*. *Appl. Environ. Microbiol.* **2014,** *80* (21), 6677-6684.

16. Liu, Z.; Inokuma, K.; Ho, S. H.; den Haan, R.; Hasunuma, T.; van Zyl, W. H.; Kondo, A., Combined cell-surface display- and secretion-based strategies for production of cellulosic ethanol with *Saccharomyces cerevisiae*. *Biotechnol. Biofuels* **2015,** *8*, 162.
17. Wachtmeister, J.; Rother, D., Recent advances in whole cell biocatalysis techniques bridging from investigative to industrial scale. *Curr. Opin. Biotechnol.* **2016,** *42*, 169-177.
18. Liu, X.; Cheng, J.; Zhang, G.; Ding, W.; Duan, L.; Yang, J.; Kui, L.; Cheng, X.; Ruan, J.; Fan, W.; Chen, J.; Long, G.; Zhao, Y.; Cai, J.; Wang, W.; Ma, Y.; Dong, Y.; Yang, S.; Jiang, H., Engineering yeast for the production of breviscapine by genomic analysis and synthetic biology approaches. *Nat. Commun.* **2018,** *9* (1), 448.
19. Liang, B.; Li, L.; Tang, X.; Lang, Q.; Wang, H.; Li, F.; Shi, J.; Shen, W.; Palchetti, I.; Mascini, M.; Liu, A., Microbial surface display of glucose dehydrogenase for amperometric glucose biosensor. *Biosens. Bioelectron.* **2013,** *45*, 19-24.
20. Liang, B.; Lang, Q.; Tang, X.; Liu, A., Simultaneously improving stability and specificity of cell surface displayed glucose dehydrogenase mutants to construct whole-cell biocatalyst for glucose biosensor application. *Bioresour. Technol.* **2013,** *147* (0), 492-498.
21. Yan, Y.; Zheng, W.; Su, L.; Mao, L., Carbon-nanotube-based glucose/O_2 biofuel cells. *Adv. Mater.* **2006,** *18* (19), 2639-2643.
22. Trifonov, A.; Herkendell, K.; Tel-Vered, R.; Yehezkeli, O.; Woerner, M.; Willner, I., Enzyme-capped relay-functionalized mesoporous carbon nanoparticles: effective bioelectrocatalytic matrices for sensing and biofuel cell applications. *ACS Nano* **2013,** *7* (12), 11358-11368.
23. Zebda, A.; Gondran, C.; Le Goff, A.; Holzinger, M.; Cinquin, P.; Cosnier, S., Mediatorless high-power glucose biofuel cells based on compressed carbon nanotube-enzyme electrodes. *Nat. Commun.* **2011,** *2*, 370.
24. Agnes, C.; Holzinger, M.; Le Goff, A.; Reuillard, B.; Elouarzaki, K.; Tingry, S.; Cosnier, S., Supercapacitor/biofuel cell hybrids based on wired enzymes on carbon nanotube matrices: autonomous reloading after high power pulses in neutral buffered glucose solutions. *Energy Environ. Sci.* **2014,** *7* (6), 1884-1888.
25. Cooney, M. J.; Svoboda, V.; Lau, C.; Martin, G.; Minteer, S. D., Enzyme catalysed biofuel cells. *Energy Environ. Sci.* **2008,** *1* (3), 320-337.
26. Elouarzaki, K.; Bourourou, M.; Holzinger, M.; Le Goff, A.; Marks, R. S.; Cosnier, S., Freestanding HRP-GOx redox buckypaper as an oxygen-reducing biocathode for biofuel cell applications. *Energy Environ. Sci.* **2015,** *8* (7), 2069-2074.
27. Mazurenko, I.; Monsalve, K.; Infossi, P.; Giudici-Orticoni, M.-T.; Topin, F.; Mano, N.; Lojou, E., Impact of substrate diffusion and enzyme distribution in 3D-porous electrodes: a combined electrochemical and modelling study of a thermostable H_2/O_2 enzymatic fuel cell. *Energy Environ. Sci.* **2017,** *10* (9), 1966-1982.
28. Szczupak, A.; Halamek, J.; Halamkova, L.; Bocharova, V.; Alfonta, L.; Katz, E., Living battery - biofuel cells operating in vivo in clams. *Energy Environ. Sci.* **2012,** *5* (10), 8891-8895.
29. Xiao, X.; Magner, E., A biofuel cell in non-aqueous solution. *Chem. Commun.* **2015,** *51* (70), 13478-13480.
30. Xiao, X.; Xia, H.-q.; Wu, R.; Bai, L.; Yan, L.; Magner, E.; Cosnier, S.; Lojou, E.; Zhu, Z.; Liu, A., Tackling the challenges of enzymatic (bio)fuel cells. *Chem. Rev.* **2019,** *119* (16), 9509-9558.

31. Hou, C.; Liu, A., An integrated device of enzymatic biofuel cells and supercapacitor for both efficient electric energy conversion and storage. *Electrochim. Acta* **2017,** *245* (Supplement C), 303-308.
32. Hou, C.; Yang, D.; Liang, B.; Liu, A., Enhanced performance of a glucose/O_2 biofuel cell assembled with laccase-covalently immobilized three-dimensional macroporous gold film-based biocathode and bacterial surface displayed glucose dehydrogenase-based bioanode. *Anal. Chem.* **2014,** *86* (12), 6057-6063.
33. Miras, I.; Schaeffer, F.; Beguin, P.; Alzari, P. M., Mapping by site-directed mutagenesis of the region responsible for cohesin-dockerin interaction on the surface of the seventh cohesin domain of *Clostridium thermocellum* CipA. *Biochemistry* **2002,** *41* (7), 2115-2119.
34. Carvalho, A. L.; Dias, F. M. V.; Nagy, T.; Prates, J. A. M.; Proctor, M. R.; Smith, N.; Bayer, E. A.; Davies, G. J.; Ferreira, L. M. A.; Romão, M. J.; Fontes, C. M. G. A.; Gilbert, H. J., Evidence for a dual binding mode of dockerin modules to cohesins. *Proc. Natl. Acad. Sci.* **2007,** *104* (9), 3089.
35. Pinheiro, B. A.; Proctor, M. R.; Martinez-Fleites, C.; Prates, J. A. M.; Money, V. A.; Davies, G. J.; Bayer, E. A.; FontesM, C. M. G. A.; Fierobe, H.-P.; Gilbert, H. J., The Clostridium cellulolyticum Dockerin Displays a Dual Binding Mode for Its Cohesin Partner. *J. Biol. Chem.* **2008,** *283* (26), 18422-18430.
36. You, C.; Chen, H.; Myung, S.; Sathitsuksanoh, N.; Ma, H.; Zhang, X.-Z.; Li, J.; Zhang, Y. H. P., Enzymatic transformation of nonfood biomass to starch. *Proc. Natl. Acad. Sci.* **2013,** *110* (18), 7182.
37. Liang, B.; Lang, Q.; Tang, X.; Liu, A., Simultaneously improving stability and specificity of cell surface displayed glucose dehydrogenase mutants to construct whole-cell biocatalyst for glucose biosensor application. *Bioresourc. Technol.* **2013,** *147* (0), 492-498.
38. Xia, L.; Liang, B.; Li, L.; Tang, X.; Palchetti, I.; Mascini, M.; Liu, A., Direct energy conversion from xylose using xylose dehydrogenase surface displayed bacteria based enzymatic biofuel cell. *Biosens. Bioelectron.* **2013,** *44* (0), 160-163.
39. Lang, Q.; Yin, L.; Shi, J.; Li, L.; Xia, L.; Liu, A., Co-immobilization of glucoamylase and glucose oxidase for electrochemical sequential enzyme electrode for starch biosensor and biofuel cell. *Biosens. Bioelectron.* **2014,** *51* (0), 158-163.
40. Fishilevich, S.; Amir, L.; Fridman, Y.; Aharoni, A.; Alfonta, L., Surface display of redox enzymes in microbial fuel cells. *J. Am. Chem. Soc.* **2009,** *131* (34), 12052-12053.
41. Liang, B.; Li, L.; Mascin, M.; Liu, A., Construction of xylose dehydrogenase displayed on the surface of bacteria using ice nucleation protein for sensitive D-Xylose detection. *Anal. Chem.* **2011,** *84* (1), 275-282.
42. Fan, S.; Hou, C.; Liang, B.; Feng, R.; Liu, A., Microbial surface displayed enzymes based biofuel cell utilizing degradation products of lignocellulosic biomass for direct electrical energy. *Bioresour. Technol.* **2015,** *192*, 821-825.
43. Feng, R.; Liang, B.; Hou, C.; Han, D.; Han, L.; Lang, Q.; Liu, A.; Han, L., Rational design of xylose dehydrogenase for improved thermostability and its application in development of efficient enzymatic biofuel cell. *Enzyme Microb. Technol.* **2016,** *84*, 78-85.
44. Wang, H. W.; Lang, Q. L.; Li, L.; Liang, B.; Tang, X. J.; Kong, L. R.; Mascini, M.; Liu, A. H., Yeast surface displaying glucose oxidase as whole-cell biocatalyst: construction, characterization, and its electrochemical glucose sensing application. *Anal. Chem.* **2013,** *85* (12), 6107-6112.

45. Guo, Y.; Lu, F.; Zhao, H.; Tang, Y.; Lu, Z., Cloning and heterologous expression of glucose oxidase gene from *aspergillus niger* z-25 in *pichia pastoris*. *Appl. Biochem. Biotechnol.* **2010,** *162* (2), 498-509.
46. de Carvalho, C. C. C. R., Enzymatic and whole cell catalysis: Finding new strategies for old processes. *Biotechnol. Adv.* **2011,** *29* (1), 75-83.
47. Li, X.; Xiao, Y.; Feng, Y.; Li, B.; Li, W.; Cui, Q., The spatial proximity effect of beta-glucosidase and cellulosomes on cellulose degradation. *Enzyme Microb. Technol.* **2018,** *115*, 52-61.
48. Wheeldon, I.; Minteer, S. D.; Banta, S.; Barton, S. C.; Atanassov, P.; Sigman, M., Substrate channelling as an approach to cascade reactions. *Nat. Chem.* **2016,** *8* (4), 299-309.
49. Kumar, P.; Satyanarayana, T., Microbial glucoamylases: characteristics and applications. *Crit. Rev. Biotechnol.* **2009,** *29* (3), 225-255.
50. Seehuber, A.; Dahint, R., Conformation and Activity of Glucose oxidase on homogeneously coated and nanostructured surfaces. *J. Phys. Chem. B* **2013,** *117* (23), 6980-6989.
51. Liang, B.; Li, L.; Mascin, M.; Liu, A., Construction of xylose dehydrogenase displayed on the surface of bacteria using ice nucleation protein for sensitive D-Xylose detection. *Anal. Chem.* **2012,** *84* (1), 275-282.
52. Le Goff, A.; Holzinger, M.; Cosnier, S., Recent progress in oxygen-reducing laccase biocathodes for enzymatic biofuel cells. *Cell. Mol. Life Sci.* **2015,** *72* (5), 941-52.
53. Amao, Y.; Sakai, Y.; Teshima, Y., Photoelectrochemical starch-O_2 biofuel cell consisting of chlorophyll derivative-sensitized TiO_2 anode and enzyme-based cathode. *Res. Chem. Intermed.* **2016,** *42* (11), 7761-7770.
54. Lang, Q.; Yin, L.; Shi, J.; Li, L.; Xia, L.; Liu, A., Co-immobilization of glucoamylase and glucose oxidase for electrochemical sequential enzyme electrode for starch biosensor and biofuel cell. *Biosens Bioelectron* **2014,** *51* (0), 158-163.
55. Kim, D. C.; Sohn, J. I.; Zhou, D.; Duke, T. A. J.; Kang, D. J., Controlled assembly for well-defined 3D bioarchitecture using two active enzymes. *ACS Nano* **2010,** *4* (3), 1580-1586.
56. Dueber, J. E.; Wu, G. C.; Malmirchegini, G. R.; Moon, T. S.; Petzold, C. J.; Ullal, A. V.; Prather, K. L. J.; Keasling, J. D., Synthetic protein scaffolds provide modular control over metabolic flux. *Nat. Biotechnol.* **2009,** *27* (8), 753-759.
57. Wheeldon, I.; Minteer, S.; Banta, S.; Barton, S.; Atanassov, P.; Sigman, M., Substrate channelling as an approach to cascade reactions. *Nat. Chem.* **2016,** *8*, 299-309.
58. Osman, M. H.; Shah, A. A.; Walsh, F. C., Recent progress and continuing challenges in bio-fuel cells. Part I: enzymatic cells. *Biosens. Bioelectron.* **2011,** *26* (7), 3087-3102.

Scheme 1

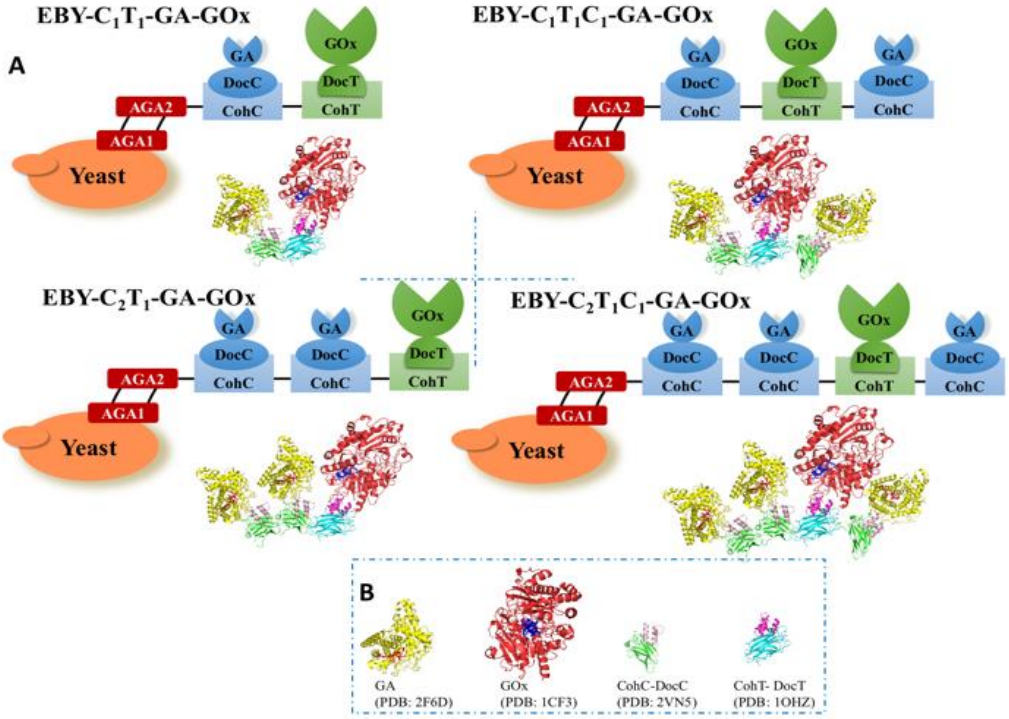
A
EBY-C1T1-GA-GOx
EBY-C1T1C1-GA-GOx
EBY-C2T1-GA-GOx
EBY-C2T1C1-GA-GOx
GA
GOx
DocC
DocT
CohC
CohT
AGA2
AGA1
Yeast
B
GA
(PDB: 2F6D)
GOx
(PDB: 1CF3)
CohC-DocC
(PDB: 2VN5)
CohT- DocT
(PDB: 1OHZ)

Figure 1

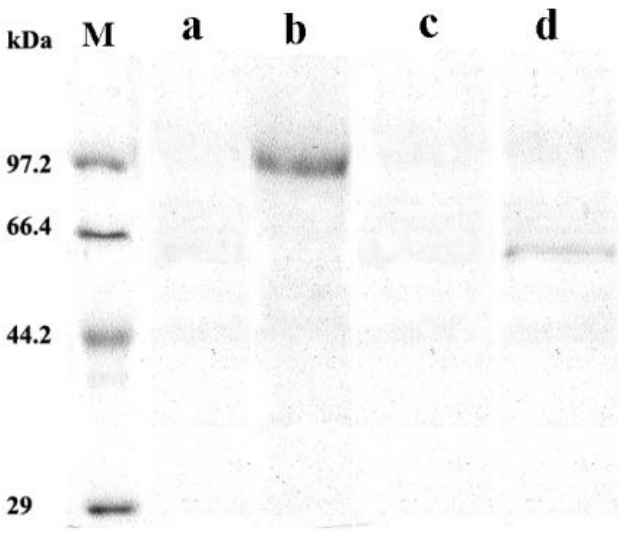

Figure 2

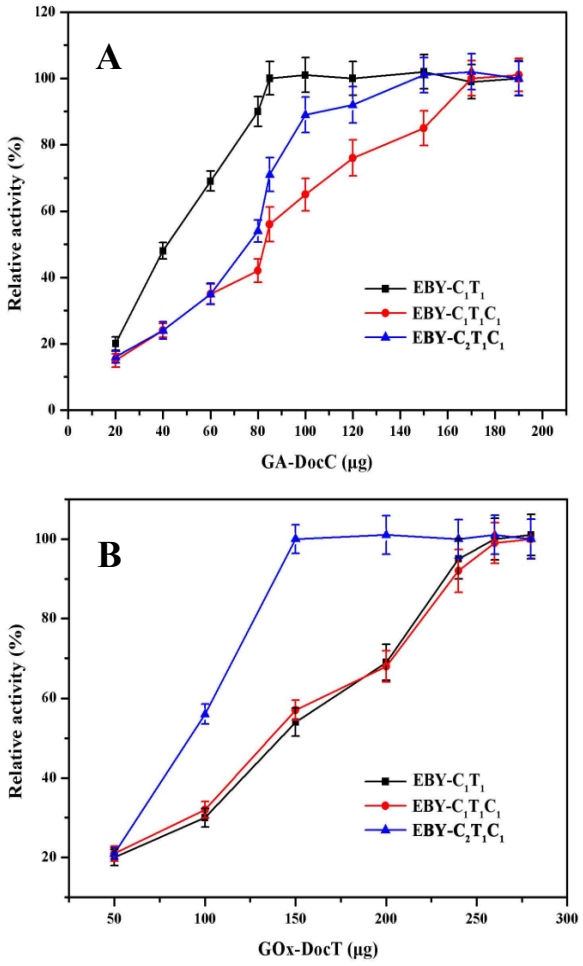
A
Relative activity (%)
GA-DocC (μg)
EBY-C1T1
EBY-C1T1C1
EBY-C2T1C1
B
Relative activity (%)
GOx-DocT (μg)
EBY-C1T1
EBY-C1T1C1
EBY-C2T1C1

Figure 3

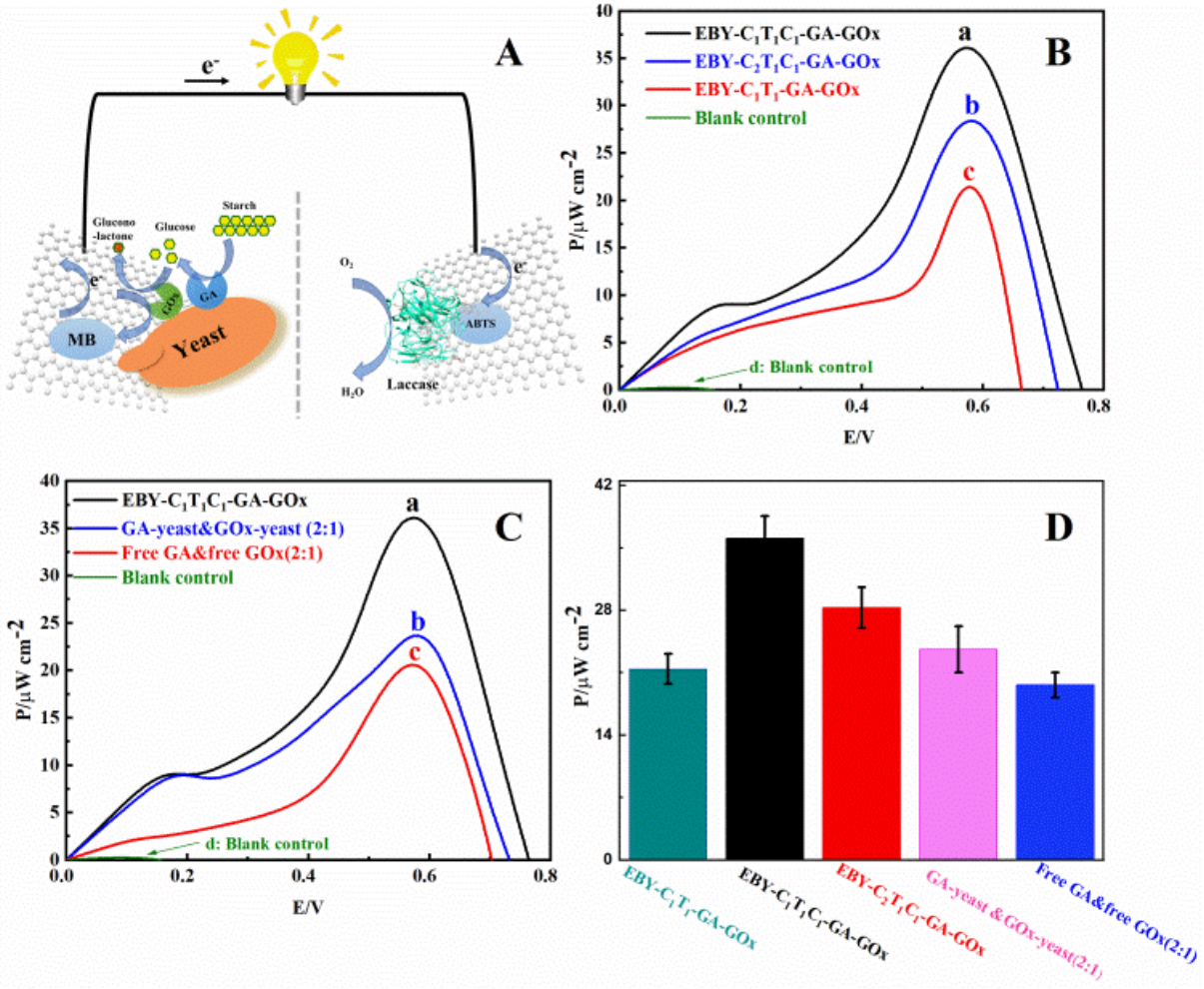
A
e⁻
Gluconolactone
Glucose
Starch
GOx
GA
MB
Yeast
e⁻
O₂
e⁻
ABTS
H₂O
Laccase
B
EBY-C1T1C1-GA-GOx
EBY-C2T1C1-GA-GOx
EBY-C1T1-GA-GOx
Blank control
a
b
c
d: Blank control
P/μW cm⁻²
E/V
C
EBY-C1T1C1-GA-GOx
GA-yeast&GOx-yeast (2:1)
Free GA&free GOx(2:1)
Blank control
a
b
c
d: Blank control
P/μW cm⁻²
E/V
D
P/μW cm⁻²
EBY-C1T1-GA-GOx
EBY-C1T1C1-GA-GOx
EBY-C2T1C1-GA-GOx
GA-yeast &GOx-yeast(2:1)
Free GA&free GOx(2:1)

Figure 4

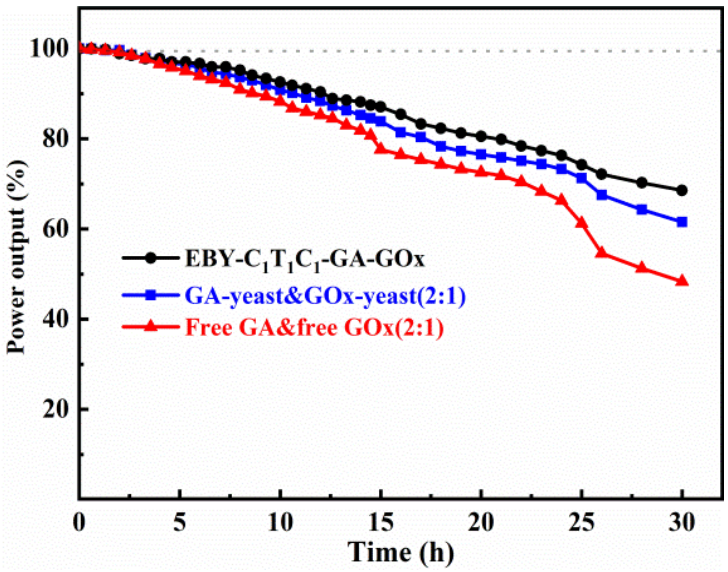
Power output (%)
100
80
60
40
20
0
5
10
15
20
25
30
Time (h)
EBY-C1T1C1-GA-GOx
GA-yeast&GOx-yeast(2:1)
Free GA&free GOx(2:1)

GRAPHIC TOC:

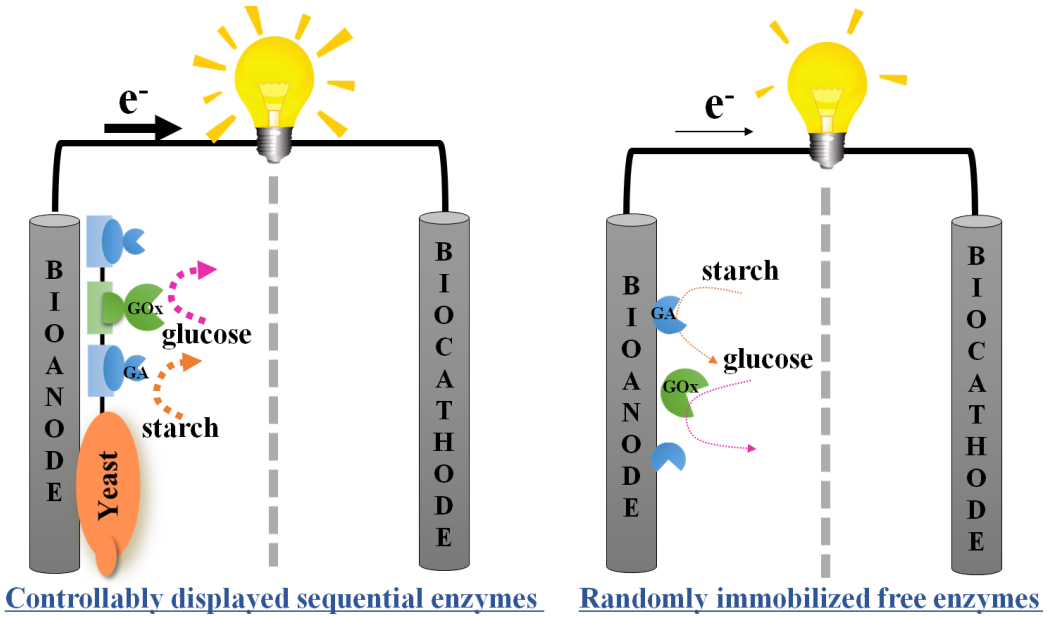

Controllably displayed sequential enzymes Randomly immobilized free enzymes